2021 43rd Annual International Conference of the
IEEE Engineering in Medicine & Biology Society (EMBC)
Oct 31 - Nov 4, 2021. Virtual Conference

A Multi-Modular System for the Visualization and Classification of MER Data During Neurostimulation Procedures

Andre Waschk[1] and Yaroslav Parpaley[2] and Jens Krüger[3]

Abstract— **This paper proposes an interactive analysis and visualization tool for the accuracy improvement of electrode placement during neurostimulation therapy surgery. During the procedure, the presented system assists the surgeon in the crucial tissue type detection by providing a fused visualization of the current electrode location and the microelectrode recordings (MER). The system processes the MER in real-time and utilizes a convolutional neural network (CNN) to classify the targeted tissue type. In addition to presenting the MER in its raw waveform, the system also offers the visualization of the frequency domain and the result of the neural network. To further assist the decision-making process, additional visualization methods are integrated into the system. Using the pre-operative taken CT and MRI scans, the system offers 3D visualization in the form of direct volume rendering (DVR) and axis-aligned slice views in 2D. Both domains are enriched by the MER readings and the result of the machine learning classifier.**

I. INTRODUCTION

Neurostimulation therapy [5] has been established itself as a suitable treatment for various movement disorders like Parkinson's disease [14], essential tremor [4], dystonia [17], or Tourette syndrome [12]. One neurostimulation procedure widely adopted in the clinical field is Deep Brain Stimulation (DBS) [13], which is used when traditional medications fail to control the symptoms. Compared to other neurosurgical procedures, for example, thalamotomy [15], DBS does not harm nerve cells and instead blocks malfunctioning signals within the target area.

To achieve the treatment of these movement disorders, DBS aims to implant an electrode within the patient's brain. The implant emits electrical impulses within a target area. A typical DBS procedure consists of three-phases, the pre-operative planning phase, the insertion of the electrode, and the postoperative care. The crucial planning phase is used to locate the target tissue for the procedure, the subthalamic nucleus (STN) [16], and determine the electrode's exact placement. Preoperatively taken CT [3] and MRI [19] scans are used to locate the tissue and translate the planned location into actual angles and penetration depth for the surgery, harming as little brain tissue as possible.

During the procedure and the insertion of the electrode, surgeons mentally fuse real-time auditive feedback about the currently penetrated brain tissue using micro-electrode-recording (MER) [2] and know preoperative images to determine the tissue type around the MER-electrode. This process is to improve the accuracy of the placement over a procedure based on the low resolution imaging data alone. In the post-operative phase, the location of the pulse emission on the MER-electrode is fine tuned to achieve the best treatment.

[1]Andre Waschk is with Faculty of High Performance Computing, University of Duisburg and Essen, Germany Andre.Waschk@uni-due.de
[2]Yaroslav Parpaley is with the Department of Neurosurgery, University Hospital Bochum, Germany Yaroslav.Parpaley@kk-bochum.de
[3]Jens Krüger is with Faculty of High Performance Computing, University of Duisburg and Essen, Germany Jens.Krueger@uni-due.de

II. PROBLEM STATEMENT & CONTRIBUTION

The current state-of-the-art DBS surgery [1] heavily relies on the surgeon's capability to build a mental model of the current electrode position and the classification of different tissue types based on the auditive and visual feedback provided by the MER.

While the actual placement technology is highly developed, supporting real-time imaging and analysis software [18] has, to the best of our knowledge, not been integrated into the procedure. Imaging has to be done in the pre-processing and planning stage of the surgery and is usually not present during the actual procedure.

During the procedure, the only visual feedback surgeons get is the waveform representation of the MER. Based on the auditive and visual representation of the MER, surgeons have to decide if the target tissue is reached. Currently, available classification software that supports the surgeons in this challenging task is still in its infancy.

The contribution of this paper is a machine learning classification system for tissue type detection based on the MER signal. Secondly, we present an integrated and interactive visualization system that fuses the preoperative imaging data with the real-time analyzed and classified MER signal.

III. TISSUE TYPE CLASSIFICATION

A. Data Acquisition

During the neurosurgical procedure, surgeons need to locate and validate the pre-operatively planned target location for the final placement of the stimulation electrode. By injecting multiple recording electrodes into the patient's brain, surgeons aim to minimize any uncertainty still present due to possible errors in imaging data. These electrodes are moved in precise and discrete steps along the preplanned trajectory towards the target location and consistently sample the brain activity. Utilizing the MER device, the brain signal is sampled at a frequency of 20 kHz. The recorded data is transmitted in real-time to the system for further processing using a direct ethernet connection between the system and the recording hardware. For each step and inserted electrode, between 7 and 15 seconds of brain activity are recorded.

978-1-7281-1178-0/21/$31.00 ©2021 IEEE

The recording starts 10 mm in front of the planned target tissue and ends 5 mm behind the target location, where the electrode is moved in 1 mm steps between recording steps.

B. Data Processing

The recorded signal of the MER device is the time-dependent brain activity of the currently penetrated tissue. To clean up the obsolete data present in the recorded signal, a low- and high-pass filter is applied, removing frequencies below 250 Hz and above 1000 Hz. Further data processing is mandatory to generate the input data for the neural network and tissue type detection. A Discrete Fourier Transformation [6] is applied to transform the data into its frequency domain. For tissue detection, the system uses frequencies between 250 Hz and 1000 Hz of the recorded 20 kHz signal, resulting in a frequency band of 750 entries.

C. Classification

To classify the tissue type of the currently recorded brain activity, the system uses a 1D Convolutional Neural Network [11]. As input for the Neural Network, the transformed data is used consisting of the 750 frequency entries.

The CNN uses one feature layer with an internal kernel size of ten values for the subsampling stage and a stride of five values between each neuron input (see Figure 1). With the selected kernel size, data stride, and an input vector size of 750 values, the resulting neural network consists of 150 weights to be trained.

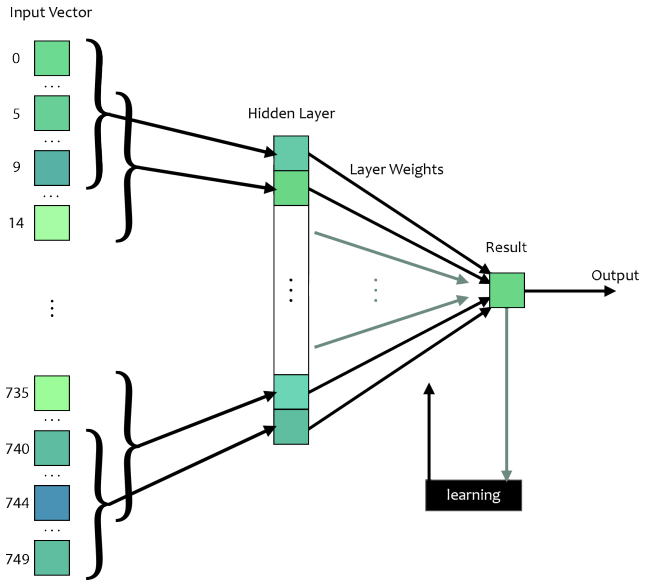

Fig. 1. The used CNN takes as input the frequency domain computed by the Fourier Transformation. For the input layer, ten frequencies are folded to a single value. The individual weights for each value are learned based on the output value and the pre-classified expected result.

For the training purpose, we selected a supervised learning approach based on the experience of highly skilled neurosurgeons. The training set consisted of data collected from 21 surgeries pre-classified by experts. Each surgery utilized six recording electrodes in total with 15 measurement points per electrode resulting in 1890 pre-determined data samples for the neural network. For Deep Brain Surgery, the network was trained to distinguish between the Subthalamic Nucleus (STN) and other tissues.

IV. VISUALIZATION

The presented system provides various visualization domains to further assist the surgeons in their task of tissue classification. The gold standard in MER-based DBS surgeries is the visualization of the recorded raw signal. The system can represent the raw data as surgeons already know them but offers visualization techniques based on the preoperative imaging data and the processed and classified brain recording. The visualization interface is separated into two domains (Figure 2), the MER-based visualization interface on the right side and the imaging-based visualization on the left.

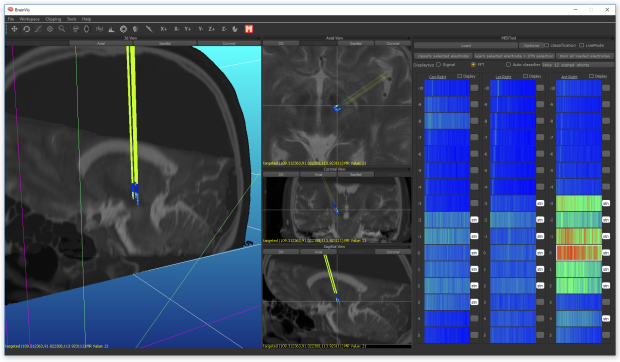

Fig. 2. The user interface of the system is separated into two spaces. The left part of the interface displays the interactive visualization of the pre-operative CT and MRI data enriched with the MER results. The right side represents the processed and analyzed MER data in real-time.

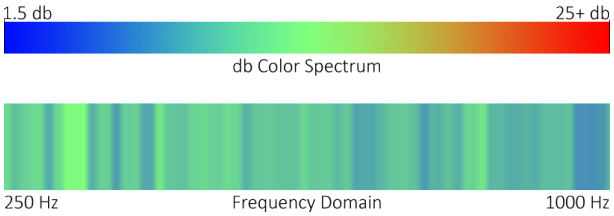

Fig. 3. The MER signal is transformed into its frequency domain. Frequencies between 250Hz and 1000 Hz are visualized within the software using the displayed color-coding.

A. MER Visualization

The MER visualization (Figure 2 right) supports the waveform representation of the recorded data and the color-coded signal in the frequency domain resulting from the Discrete Fourier Transformation (Figure 3). The X-Axis of these images represents the different frequencies considered for the classification ranging from 250 Hz to 1000 Hz. The color spectrum goes from blue over green to red, where blue indicates the lowest amplitudes and red the highest amplitudes. The system processes the incoming data in real-time,

and the result of the trained CNN is immediately displayed next to each recording set providing direct feedback to the neurosurgeon. By displaying all recordings taken during the session with the addition of the classification simultaneously, the neurosurgeon gains a quick overview of the complete implantation at a glance (Figure 5).

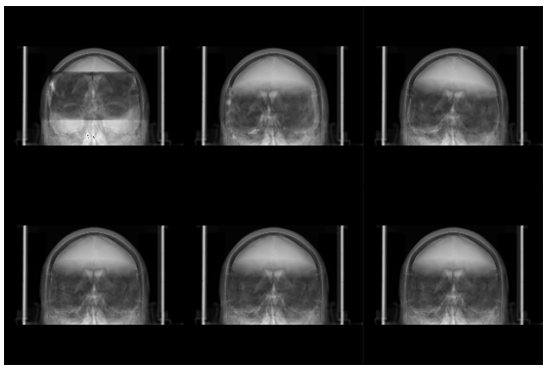

Fig. 4. Using the GPU accelerated method based on a gradient descent approach the system automatically fuses the MRI and CT images in milliseconds. Top left: starting position; Bottom right: Final registration.

B. Fused Visualization

To improve the decision-making process, the system adds the pre-operatively taken MRI and CT imaging data as 2D axis-aligned slice views and 3D volume data.

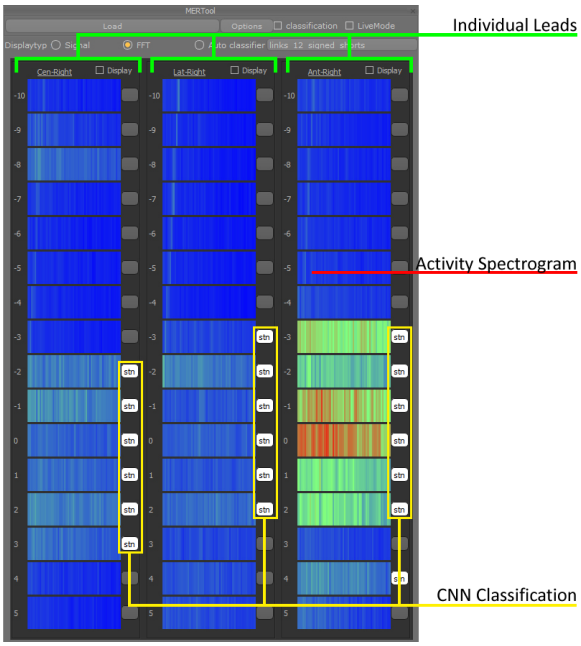

Fig. 5. Close-up of the MER-Widget: The number of displayed columns depends on the number of used recording leads. The tool allows switching between the visualization of the spectrogram and waveform. The automatic classification is displayed in real-time next to each recording.

The visualization of these two data-set domains has to fulfill several constraints to complement intraoperative use. The CT and MRI scans have to be registered against each other to locate the correct target tissues. This process can be costly and often requires manual adjustments by neurosurgeons. The presented system utilizes a fully automatic registration technique designed for this use case utilizing modern GPU features and determines the best suitable position within milliseconds with a gradient descent approach (Figure 4).

In contrast to the visualization of the 2D axis-aligned slices, the visualization of 3D volumes can be very computationally expensive. For intraoperative use, the visualization has to be interactive and responsive to the user. The system uses state-of-the-art direct volume rendering with several acceleration techniques [9], [7] to guarantee a fluid interaction with the data set. By adding multiple clipping techniques and windowing functions [10], neurosurgeons are already familiar with the system can be used intuitively during the procedure.

The neurosurgeons can cross-validate the result of the automatic tissue type classifier within the 2D and 3D visualization. The results are rendered as geometric primitives at the corresponding location of the MER data (Figure 6) and are color-coded by the average amplitude found.

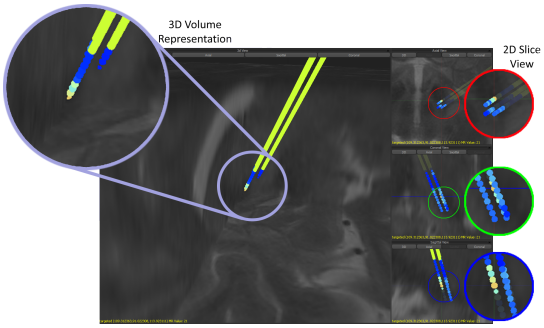

Fig. 6. The classified MER data is represented in the 3D and 2D visualization of the system. Surgeons can cross-validate the findings using the pre-operative imaging data and the intraoperative recordings.

V. RESULTS

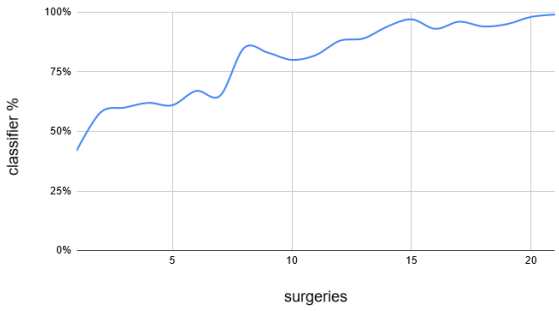

Fig. 7. The CNN got trained after every surgery with new data. After each training session, the best-trained network was used for the upcoming procedure. After 14 sessions the network reached a consistent classification of 90%.

The neural network of the system was trained using a supervised learning approach. We collected data from weekly procedures and the manual classification of the corresponding neurosurgeon for the training purpose. In total, 1890 pre-classified recordings were gathered, ranging between 8 and

13 seconds. To enhance the robustness of the network, next to the frequency domain computed over the entire recording additional 5-second windows were randomly selected to further expand the training set. As result, the complete training set consisted of 3780 frequency bands.

Successively more samples were added to the training set until the number above was reached. The weights of the neuronal network were adjusted after all currently available samples were evaluated using backpropagation. The final neural network is the result of multiple generations fine-tuned over multiple procedures. As displayed in Figure 7 the best network reached a validation rate of 98.6% for the STN.

VI. CONCLUSION

In this paper, we presented an assistance system for neurostimulation surgeries. The system presents two different domains that support surgeons in their complex tasks during the procedure. The first domain is the analysis and automatic classification of the MER data. We provide a Convolutional Neural Network trained to classify the Subthalamic Nucleus in real-time with very high certainty and present a straightforward visualization for intraoperative use.

The second domain of the system is the visualization of the imaging-based from the preoperative CT and MRI scans. We integrated this domain to enhance tissue type detection further and provide an additional feedback channel to the surgeon. The 2D axis-aligned slice view and the 3D direct volume rendering of both scans support fast and reliable dataset registration and visualization for interaction. The result of the MER analysis supplements the visualization and allows the surgeon to cross-validate their assessment of the situation.

VII. DISCUSSION

The presented system was constructed and developed in close relationship with neurosurgeons in clinical practice. It received very positive feedback for its ease of use and the additional insight provided by its classification and visualization.

The used neural network was trained to achieve a very high validation rate at minimal complexity. In its current state, the network was trained based on pre-classified data only to detect the STN but can not distinguish other tissue types. For the future and other procedures, we intend to train the network for additional tissue types.

For other neurostimulation therapies, where MER is not used to detect the target area, additional inputs have to be considered, like motor neuron activity or patient task performance. These data types can also be used as input for a neural network and cross-visualized for more certainty during the procedure.

Currently, the system uses direct volume rendering to visualize the CT and MRI scans as a cross-validation layer for the neurosurgeon. In crucial procedures like DBS, fiber tracks computed from DTI [8] could significantly supplement the visualization and be straightforward to be added to our system.

REFERENCES

[1] S. Breit, J. B. Schulz, and A.-L. Benabid. Deep brain stimulation. *Cell and Tissue Research*, 318(1):275–288, 2004.

[2] L. G. Brock, J. S. Coombs, and J. C. Eccles. The recording of potentials from motoneurones with an intracellular electrode. *The Journal of Physiology*, 117(4):431–460, 1952.

[3] T. M. Buzug. *Computed Tomography*, pages 311–342. Springer Berlin Heidelberg, Berlin, Heidelberg, 2011.

[4] S. Groppa, J. Herzog, D. Falk, C. Riedel, G. Deuschl, and J. Volkmann. Physiological and anatomical decomposition of subthalamic neurostimulation effects in essential tremor. *Brain*, 137(1):109–121, 11 2013.

[5] R. E. Gross and A. M. Lozano. Advances in neurostimulation for movement disorders. *Neurological Research*, 22(3):247–258, 2000.

[6] H. Kaptan, M. Ayaz, and H. Ekmekçi. Effect transformation of the micro electrode recording (mer) data to fast fourier transform (fft) for the main target nucleus determination for stn-dbs. *Acta informatica medica : AIM : journal of the Society for Medical Informatics of Bosnia & Herzegovina : casopis Drustva za medicinsku informatiku BiH*, 22(6):411–412, 12 2014.

[7] J. Krüger and R. Westermann. Acceleration techniques for gpu-based volume rendering. In *Proceedings of the 14th IEEE Visualization 2003 (VIS'03)*, VIS '03, page 38, USA, 2003. IEEE Computer Society.

[8] D. Le Bihan, J.-F. Mangin, C. Poupon, C. A. Clark, S. Pappata, N. Molko, and H. Chabriat. Diffusion tensor imaging: Concepts and applications. *Journal of Magnetic Resonance Imaging*, 13(4):534–546, 2001.

[9] M. Levoy. Efficient ray tracing of volume data. *ACM Trans. Graph.*, 9(3):245–261, July 1990.

[10] P. Ljung, J. Krüger, E. Gröller, M. Hadwiger, C. D. Hansen, and A. Ynnerman. State of the Art in Transfer Functions for Direct Volume Rendering. *Computer Graphics Forum*, 2016.

[11] K. O'Shea and R. Nash. An introduction to convolutional neural networks, 2015.

[12] N. Pedroarena-Leal and D. Ruge. Toward a symptom-guided neurostimulation for gilles de la tourette syndrome. *Frontiers in Psychiatry*, 8:29, 2017.

[13] J. S. Perlmutter and J. W. Mink. Deep brain stimulation. *Annual Review of Neuroscience*, 29(1):229–257, 2006. PMID: 16776585.

[14] W. Schuepbach, J. Rau, K. Knudsen, J. Volkmann, P. Krack, L. Timmermann, T. Hälbig, H. Hesekamp, S. Navarro, N. Meier, D. Falk, M. Mehdorn, S. Paschen, M. Maarouf, M. Barbe, G. Fink, A. Kupsch, D. Gruber, G.-H. Schneider, E. Seigneuret, A. Kistner, P. Chaynes, F. Ory-Magne, C. Brefel Courbon, J. Vesper, A. Schnitzler, L. Wojtecki, J.-L. Houeto, B. Bataille, D. Maltête, P. Damier, S. Raoul, F. Sixel-Doering, D. Hellwig, A. Gharabaghi, R. Krüger, M. Pinsker, F. Amtage, J.-M. Régis, T. Witjas, S. Thobois, P. Mertens, M. Kloss, A. Hartmann, W. Oertel, B. Post, H. Speelman, Y. Agid, C. Schade-Brittinger, and G. Deuschl. Neurostimulation for parkinson's disease with early motor complications. *New England Journal of Medicine*, 368(7):610–622, 2013. PMID: 23406026.

[15] P. R. Schuurman, D. A. Bosch, P. M. Bossuyt, G. J. Bonsel, E. J. van Someren, R. M. de Bie, M. P. Merkus, and J. D. Speelman. A comparison of continuous thalamic stimulation and thalamotomy for suppression of severe tremor. *New England Journal of Medicine*, 342(7):461–468, 2000. PMID: 10675426.

[16] F. Steigerwald, L. Müller, S. Johannes, C. Matthies, and J. Volkmann. Directional deep brain stimulation of the subthalamic nucleus: A pilot study using a novel neurostimulation device. *Movement Disorders*, 31(8):1240–1243, 2016.

[17] M. Vidailhet, L. Vercueil, J.-L. Houeto, P. Krystkowiak, A.-L. Benabid, P. Cornu, C. Lagrange, S. Tézenas du Montcel, D. Dormont, S. Grand, S. Blond, O. Detante, B. Pillon, C. Ardouin, Y. Agid, A. Destée, and P. Pollak. Bilateral deep-brain stimulation of the globus pallidus in primary generalized dystonia. *New England Journal of Medicine*, 352(5):459–467, 2005. PMID: 15689584.

[18] A. Waschk, Y. Parpaley, and J. Krüger. An integrated system for analysis and visualization of neurostimulation procedures. In *Proceedings of the Supercomputing Workshop on Medical Image Analysis and Visaulization*, 2016.

[19] S. W. Young. *Magnetic resonance imaging: Basic principles*. Raven Press, United States, 1987.